www.sciencemag.org/content/348/6233/457/suppl/DC1

Supplementary Materials for

Mechanical force releases nascent chain–mediated ribosome arrest in vitro and in vivo

Daniel H. Goldman, Christian M. Kaiser,* Anthony Milin, Maurizio Righini, Ignacio Tinoco Jr., Carlos Bustamante*

*Corresponding author. E-mail: carlos@alice.berkeley.edu (C.B.); kaiser@jhu.edu

Published 24 April 2015, *Science* **348**, 457 (2015)
DOI: 10.1126/science.1261909

This PDF file includes:

Materials and methods:

Preparation of SecM-stalled RNCs for optical tweezers experiments

Stalled RNCs with covalently attached dsDNA oligonucleotides and N-terminally biotinylated nascent chains were prepared using the PURExpress Δ Ribosome Kit (New England Biolabs) as described (*11*) with several modifications. Instead of truncated mRNAs, RNCs were stalled at the SecM sequence. After the initial translation reaction, RNCs were treated with 40 μM puromycin, to release nascent chains that were not SecM-stalled. RNCs were sedimented through a 1 M sucrose cushion in a polymix buffer containing 20 mM HEPES-KOH pH 7.5, 5 mM $MgCl_2$, 0.5 mM $CaCl_2$, 5 mM NH_4Cl, 95 mM KCl, 1 mM spermidine, 8 mM putrescine, 0.1 mM DTT, 0.01 mM PMSF and 0.1 mM benzamidine, and stored at -80°C in the same buffer until the day of experiments.

Optical tweezers experiments with SecM-stalled RNCs

Immediately before experiments, SecM-stalled RNCs modified with a covalently attached dsDNA oligonucleotide were ligated to a dsDNA oligonucleotide on a polystyrene microsphere, as described (*11*).

To make the DNA "handle" bead needed for forming tethers, an ~2kb dsDNA was synthesized by PCR with a forward primer labeled with a biotin molecule and a reverse primer labeled with two digoxigenin molecules. The second digoxigenin provides additional mechanical stability when the tether is brought under tension. Anti-digoxigenin coated beads were incubated at room temperature with the biotin/digoxigenin labeled dsDNA, then with streptavidin, before injection into the optical tweezers chamber. Tethers were formed by bringing the two beads in close proximity to each other. Optical tweezers experiments were performed in a polymix buffer containing 20 mM HEPES-KOH pH 7.5, 5 mM $MgCl_2$, 0.5 mM $CaCl_2$, 5 mM NH_4Cl, 95 mM KCl, 1 mM spermidine, 8 mM putrescine, 0.1 mM DTT, 0.01 mM PMSF and 0.1 mM benzamidine, and either in the presence or absence of puromycin, EF-G and GTP.

Only tethers displaying the reversible "hopping" signature of the CaM nascent chain at ~7pN were considered, ensuring tethering of the desired RNCs. After a tether was identified, the force was raised to the force of interest. During data analysis, the time between raising the force and tether rupture was recorded. If tethers displayed any

unexpected extension changes during the measurement, the molecule was not included in the analysis, as such extension changes might indicate mechanical disruption of some portion of the assembly.

The rupture lifetimes were well described by a single-exponential, as expected for a single rate-determining step for the reaction. At forces below 30 pN, a fraction of the molecules had not ruptured by our cutoff time of 10 min. We used a right-censoring, single-exponential maximum-likelihood estimator (MLE) (*28*) to calculate the time constant for stalling. The reported rates of release are the reciprocals of the time constants. We fit the force-dependent rates to Bell's model (*15*): $k(F) = k_0 \mathrm{e}^{\Delta x^{\ddagger} \mathrm{F}/\mathrm{k}_B T}$ with F = force, k_B = Boltzmann constant, T = absolute temperature.

Puromycin, EF-G and GTP concentration in optical tweezers experiments

For optical tweezers experiments, we used puromycin dihydrochloride from Sigma-Aldrich. According to the manufacturer, λ_{max} = 266-270 nm and ε = 18.5-20.5 $cm^{-1}mM^{-1}$. Using the middle value for both parameters (λ_{max} = 268 nm and ε = 19.5), we estimate our puromycin concentration at 411 μM. Using the Michaelis-Menten parameters for puromycin reactivity of the posttranslocation state (*29*), we estimate a rate of 1.9 s^{-1} for the puromycin reaction, several orders of magnitude faster than the restart rates measured in the optical tweezers experiments.

EF-G was added to a final concentration of 1 μM. Using the Michaelis-Menten parameters for EF-G catalyzed translocation (*30*), we estimate a rate of 1.1 s^{-1} for translocation, also several orders of magnitude faster than measured restart rates. GTP was added to a final concentration of 1 mM.

In vivo arrest release

Plasmids for expression of the GFP reporter constructs shown in Figure 2A were generated in the following way: Oligonucleotides encoding linker sequences from 4 to 28 amino acids in length connecting Top7 and SecM17 were assembled as shown in Figure S7. A plasmid was created that encodes Top7, SecM17 and GFPuv under the control of a T7 promoter. SapI restriction sites were introduced near the 3' end of the Top7 coding

sequence and near the 5' end of the SecM17 coding sequence. Digestion of this plasmid with SapI leaves 3-nucleotide overhangs that are compatible with the terminal overhangs of the oligonucleotides encoding the linker sequences. Thus, the procedure yields a collection of plasmids that encode Top7 followed by a 4 - 28 amino acid linker sequence (in one amino acid increments; see Figure S7 for details) that connects to the SecM17 sequence followed by GFPuv.

The plasmid collection was transformed into Lemo21(DE3) cells (New England Biolabs) according to the manufacturer's instructions. Transformed bacteria were spread on LB agar plates containing 100 μg/ml ampicillin (for maintenance of the Top7-SecM17-GFP expression construct), 30 μg/ml chloramphenicol (for maintenance of the Lemo system) and 500 μM of each isopropyl β-D-1-thiogalactopyranoside and L-rhamnose to induce expression at appropriate levels. Colonies were grown for 30-40 hours at room temperature and plates were imaged under UV-illumination. A fraction of the clones exhibited green fluorescence. Blue autofluorescence was observed for colonies that did not exhibit green fluorescence.

We analyzed plasmid DNA sequences for a set of colonies that were picked based on their green fluorescence under UV illumination (Figure 2D). To obtain the distribution of linker lengths irrespective of green fluorescence (Figure S9), we picked colonies after growing them under repressive conditions. For analysis of plasmid DNA, individual colonies were subjected to colony PCR using primers that bind in the T7 promoter region of the plasmid (forward primer) and in the GFPuv coding sequence (reverse primer), generating PCR products of ~900 bp in size. PCR products were subjected to standard DNA sequencing. Sequencing reads covered the sequences encoding Top7, the linker region, the SecM stalling sequence, and the N-terminal region of GFP. The linker lengths reported in Figures 2D and S9 were determined from this sequence information.

Optical tweezers force ramp experiments for Top7

The Top7 open reading frame was subcloned into a vector with an N-terminal Avi-tag and a C-terminal ybbR tag. Top7 was expressed, purified, derivatized and attached to polystyrene beads as described (*11*). To make the second bead needed for

forming tethers, an ~2kb biotinylated dsDNA strand was synthesized on the bead in a PCR-like reaction as described (*11*). These beads were incubated with streptavidin before injection into the optical tweezers chamber. Tethers were formed by bringing the beads in close proximity to each other. Experiments were performed in 25 mM HEPES-KOH pH 7.5, 150 mM KCl and 5 mM $Mg(OAc)_2$.

Observed contour length of Top7 in optical tweezers experiments

The identity of Top7 in single-molecule pulling experiments was confirmed by the contour length of the molecule calculated from observed folding and unfolding transitions. Applying the worm-like chain model to our experimental data, we calculated a contour length of 35.0 ± 2.3 nm (SD) for folding, and 33.7 ± 1.4 nm (SD) for unfolding. The expected contour length is 0.365 nm/aa × 93 aa = 33.9 nm.

Transformation of folding force histogram to force-dependent rates

In order to extract the force-dependent folding rates from the folding force histogram for Top7, we modified equation [10] (*19*) (originally prescribed for unfolding) for folding. Rates were calculated by changing the limits of integration and imposing a negative pulling velocity to account for the relaxation of the polypeptide from longer to shorter extensions.

Transformation of right-censored unfolding force histogram to force-dependent rates

To determine force-dependent unfolding rates from the unfolding force histogram for Top7, we modified equation [10] (*19*) for a right-censored unfolding distribution. Modification of the theory was necessary because we only sampled a portion of the unfolding distribution in our force ramp experiments, in order to avoid tether rupture at high forces. Thus, for a fraction of force ramp pulling cycles, we did not observe an unfolding event. In such a case, the unfolding event was classified as occurring at a force higher than the maximum force sampled in the experiment. In calculating the force dependent rates according to equation [10], we included these events in the summation term. Rates were only calculated for forces less than the maximum force.

Estimating the effective stall release rate, $k_{Reff}(F)$

As opposed to the scenario on the ribosome in which the nascent protein is tethered only by its C-terminus and excluded from the tunnel, a protein tethered by both termini can be mechanically denatured from either end. Thus, the force needed to unfold the protein when pulling it from both ends will represent a lower bound for the force required when the molecule is only tethered by one end and excluded from the tunnel. Similarly, the force developed by the folding protein in the optical tweezers geometry represents a lower bound for that generated by the nascent chain on the ribosome. Additionally, a fraction of ribosomes are likely inactive and are not released from stalling by the application of force in the optical tweezers; thus, we expect that the determined release rates represent an underestimate of the true values. For both of the aforementioned reasons, the calculated rate of release in response to folding likely underestimates the rate in vivo.

Approximate solution for $k_{Reff}(F)$ assuming equilibrium between N and U

An approximate solution for $k_{Reff}(F)$, assuming equilibrium between N and U, is valid for $k_U >> k_R$. This condition is satisfied for the relevant force range (see Figure S11). The set of time-dependent differential equations describing the kinetic scheme is:

$$\frac{\partial U(t,F)}{dt} = -k_N(F) \times U(t,F) - k_0 \times U(t,F) + k_U(F) \times N(t,F)$$
$$\frac{\partial N(t,F)}{dt} = -k_U(F) \times N(t,F) - k_R(F) \times N(t,F) + k_N(F) \times U(t,F)$$
$$\frac{\partial R(t,F)}{dt} = k_R(F) \times N(t,F) + k_0 \times U(t,F)$$

Because $k_U >> k_R$ for the force range under consideration, we can define: $K_{eq} = \frac{k_N(F)}{k_U(F)}$

Using this K_{eq}, $\frac{\partial U(t,F)}{dt}$ can be expressed solely as a function of $U(t,F)$ and we can integrate with respect to time to find the solution for $U(t,F)$:

$$U(t,F) = U(0,F)e^{-k_0 t}$$

And similarly, for $N(t,F)$:

$$N(t,F) = N(0,F)e^{-k_R(F)t}$$

Substituting these expressions and K_{eq} into the expression for $\frac{\partial R(t,F)}{dt}$:

$$\frac{\partial R(t,F)}{dt} = N(0,F)[k_R(F)e^{-k_R(F)t} + \frac{k_0}{K_{eq}}e^{-k_0 t}]$$

Because we are interested in the initial rate of entry to "R", we evaluate at $t = 0$:

$$\frac{\partial R(0,F)}{dt} = N(0,F)[k_R(F) + \frac{k_0}{K_{eq}}]$$

The generic rate law is of the form:

$$\frac{\partial R(0,F)}{dt} = \mathrm{k}_{Reff}(F) \times [N+U]$$

Thus, to get $\mathrm{k}_{Reff}(F)$, we divide $\frac{\partial R(0,F)}{dt}$ by $[N+U]$ and simplify:

$\mathrm{k}_{Reff}(F) = f_0(k_R + \frac{k_U k_0}{k_N})$, where $f_0$is the fraction of natively folded protein.

Exact solution for $\mathrm{k}_{Reff}(F)$

The effective release time, $\tau_{Reff}(F)$, can be expressed as an infinite sum over all possible paths to reach the released state, with the time of each path weighted by the probability of taking that path. Since the released state can be reached either from the unfolded state via the spontaneous process, or from the folded state via the force-

dependent process, there are two sum terms. Here, we assume the protein starts in the unfolded state, although since $k_U(F) >> k_R(F)$ over the force range considered, the results do not depend significantly on the initial state of the protein.

$$\tau_{Reff}(F) = \sum_{i=0}^{\bowtie} p_1[(1-p_1)(1-p_2)]^i\,[i(\tau_U+\tau_N)+\tau_U] + \sum_{i=0}^{\bowtie} p_2(1-p_1)^{i+1}(1-p_2)^i\,[(i+1)(\tau_U+\tau_N)]$$

Here, p_1 is the branching probability for transiting from the unfolded state to the released state, and p_2 is the branching probability for transiting from the folded state to the released state:

$$p_1 = \frac{k_0}{k_0 + k_N}$$
$$p_2 = \frac{k_R}{k_R + k_U}$$

τ_U and τ_N are the lifetimes of the unfolded and folded states, respectively:

$$\tau_U = \frac{1}{k_0 + k_N}$$
$$\tau_N = \frac{1}{k_U + k_R}$$

The sums converge to give:

$$\tau_{Reff}(F) = \frac{k_N + k_R + k_U}{k_0(k_U + k_R) + k_R k_N}$$

Thus,

$$\mathrm{k}_{Reff}(F) = \frac{1}{\tau_{Reff}(F)} = \frac{k_0(k_U + k_R) + k_R k_N}{k_N + k_R + k_U}$$

This expression simplifies to the approximate solution (see section above) in the limit $k_U >> k_R$.

Figure S1. Primary sequence diagram for optical tweezers experiments. The C-terminus of CaM is positioned 58 aa residues downstream of the peptidyl-tRNA at the point of SecM stalling, allowing the domain to emerge from the ribosome exit tunnel and away from the surface of the ribosome. The arrow indicates the stalling position of ribosomes on the mRNA template. Following the terminal stalling proline, there are 34 sense codons and a stop codon.

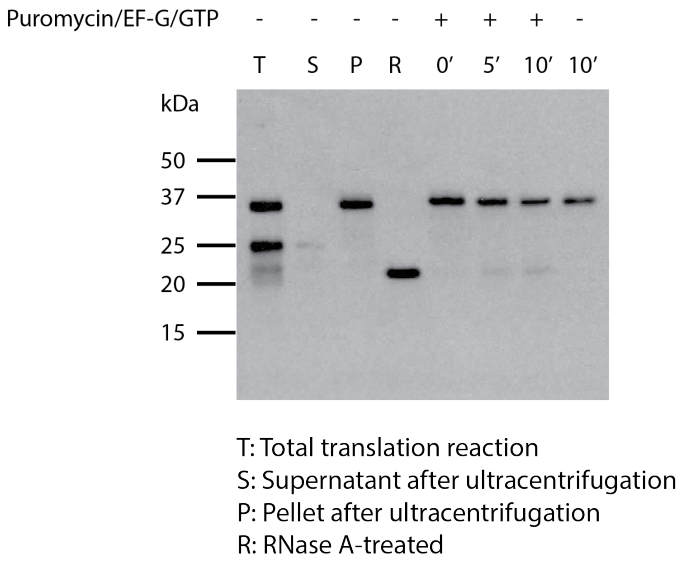

Figure S2. Preparation of SecM-stalled ribosomes. Stalled ribosomes were prepared in an *in vitro* translation system (PURE Express, NEB). Ribosomes were pelleted for 40 minutes at 200,000 g. The pellet was re-dissolved in polymix buffer and allowed to react with puromycin, EF-G and GTP or RNaseA for 10 minutes. The upper band is RNase-sensitive, indicating it is a peptidyl-tRNA species and is ribosome-bound. However, the same band is resistant to puromycin, indicating that it represents a SecM-stalled nascent chain. Nascent chains are biotinylated via an Avi tag at the N-terminus of the protein and are detected by western blotting with a streptavidin-horseradish peroxidase probe after PAGE gel electrophoresis.

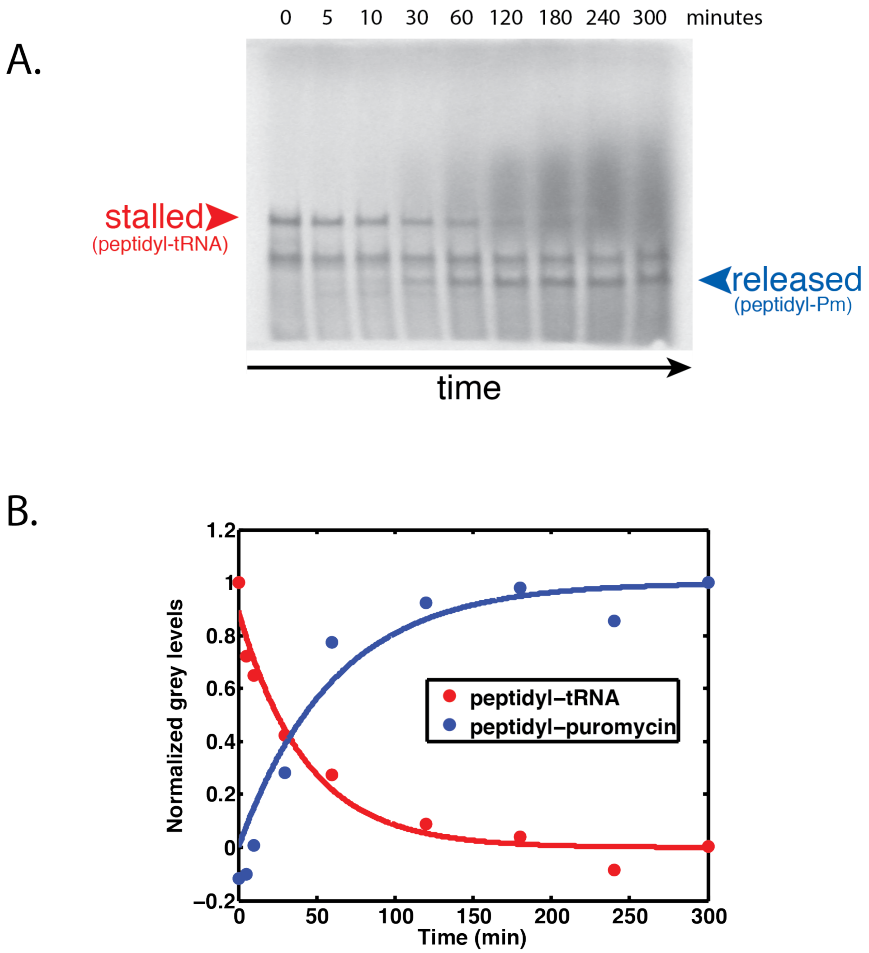

Figure S3. Arrest release of SecM-stalled ribosomes in bulk after prolonged time. **(A)** Bulk arrest release assay in the absence of force. In an initial translation reaction using the PURE system, nascent chains are ^{35}S-labeled and ribosomes translate to the SecM stall site. The reaction is then diluted into a polymix buffer containing 1 mM GTP, 1 µM EF-G and 500 µM puromycin. Arrest release is apparent as conversion of peptidyl-tRNA to peptidyl-puromycin in a gel-shift assay. **(B)** Fit of the peptidyl-tRNA to a single-exponential decay function, and the peptidyl-puromycin to a single exponential cumulative distribution function. The reported rate of $(3.9 \pm 0.1)\times10^{-4}$ s^{-1} (SEM) is the mean rate of peptidyl-tRNA decay determined from three independent experiments.

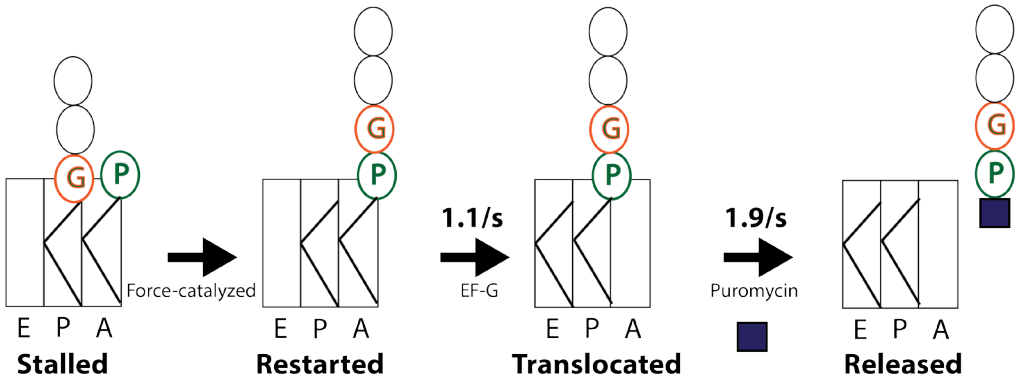

Figure S4. Schematic for the optical tweezers experiment showing A, P and E sites of the ribosome. Initially, SecM-stalled RNCs are resistant to treatment with puromycin. In the optical tweezers, force is applied to the nascent chain, catalyzing peptidyl transfer of the nascent polypeptide to the prolyl-tRNA^{pro} in the A site of the ribosome. Translocation is then catalyzed by EF-G, freeing the A site for reactivity with puromycin. The puromycin reaction leads to tether rupture. The observed time for tether rupture in the optical tweezers is a convolution of three reactions in series; however, the last two steps are very fast compared to the measured times. The rates shown for the EF-G and puromycin reactions are calculated from Michaelis-Menten parameters (*29*, *30*).

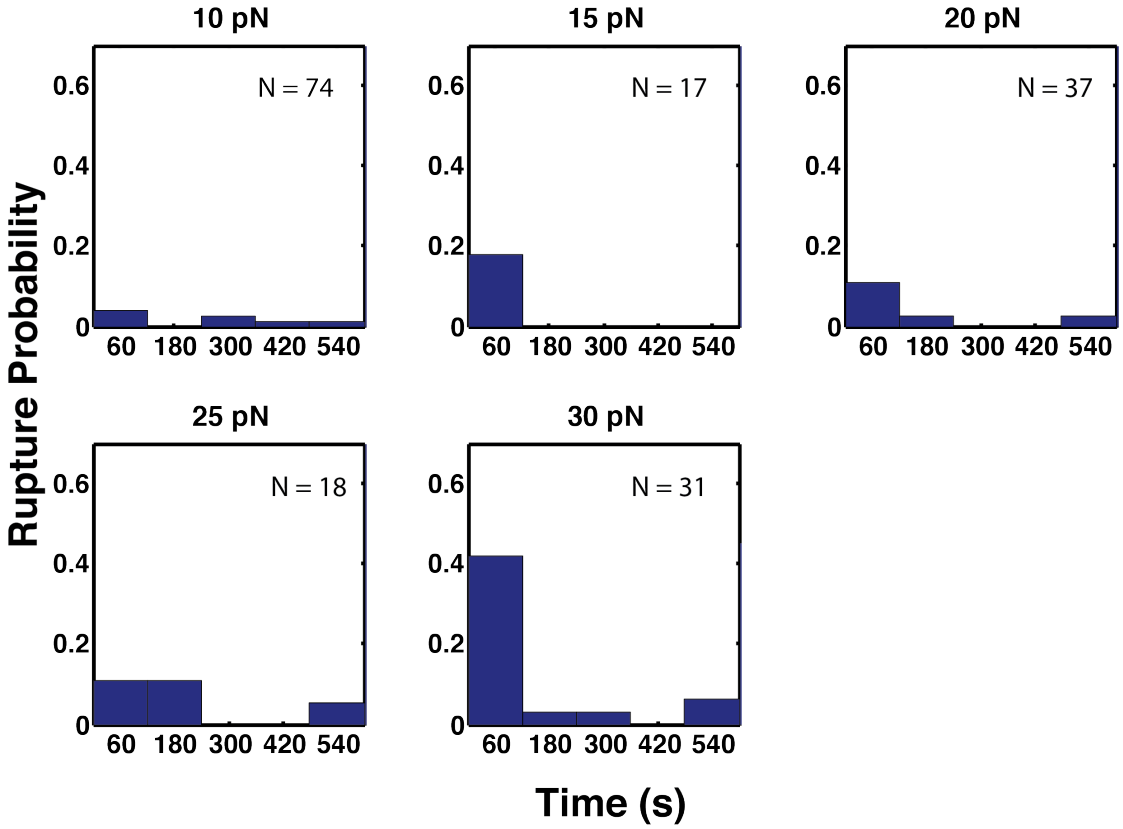

Figure S5. Control experiments in the absence of puromycin, EF-G and GTP (polymix buffer only) revealed a low rate of background rupture due to breakage of the molecular assembly for reasons other than stalling rescue.

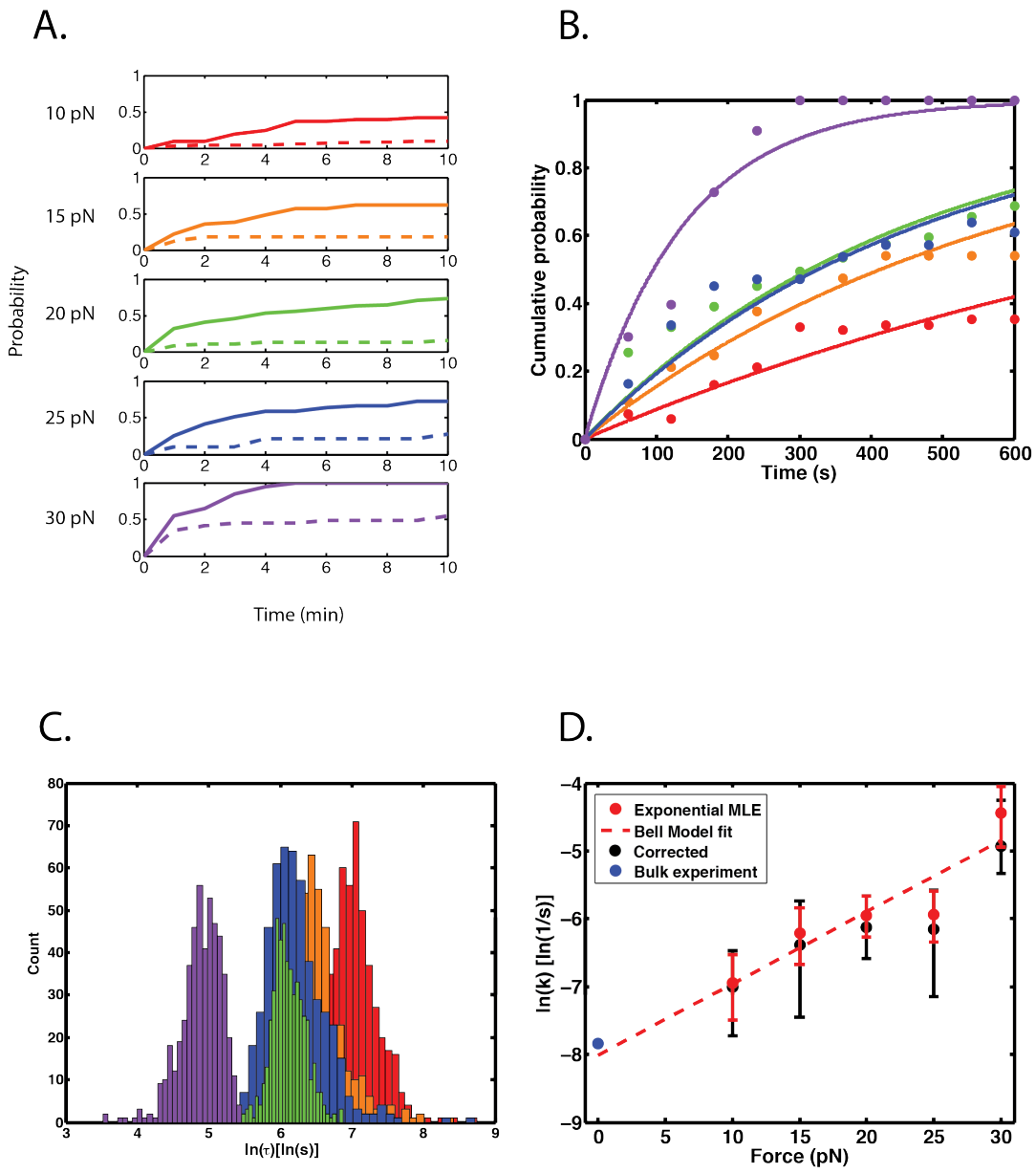

Figure S6. Alternative method for calculating force-catalyzed arrest release rates takes into account non-specific tether rupture. Correcting for nonspecific rupture events did not significantly affect the measured rates. **(A)** Cumulative probability distributions for tether rupture at each force in puromycin/EF-G/GTP (solid lines) or buffer only (dashed lines). **(B)** Cumulative rupture probability curves are re-plotted, this time taking into account non-specific rupture probability. The buffer-only distributions are subtracted from the puromycin/EF-G/GTP distributions at each respective force, and the resulting curves are re-normalized by the probability of tether survival in the buffer-only case. The resulting

distributions are fit to a single-exponential cumulative distribution function to determine the force-dependent lifetimes. Color coding as in (A) **(C)** Error is determined by bootstrapping. At each force, N lifetimes are drawn from the pool of experimentally measured lifetimes at that force, where N is the number of measurements in the data set. In this sampling process, each lifetime that is drawn is subsequently replaced in the pool of lifetimes, so it is possible to sample each point more than once (sampling with replacement). This new set of lifetimes represents a bootstrapped dataset, and is done for both the puromycin/EF-G/GTP condition and the buffer-only condition. Curves are re-normalized and fit to extract the lifetime, as described in (A). This procedure is repeated 500 times at each force, and the resulting lifetimes are plotted in a histogram. Color coding as in (A) **(D)** Comparison of rates determined by MLE fitting (red) and the method described here (black). Blue dot: Rate of release measured in bulk in the absence of force.

A.

```
>I1
5'-cggtaacggtagaaggccagctggaaggatcc-3'
   3'-attgccatcttccggtcgaccttcctaggccac-5'
      V  T  V  E  G  Q  L  E  G  S

>I2
5'-cggtaacggtagaaggccagctggaaggtggatcc-3'
   3'-attgccatcttccggtcgaccttccacctaggccac-5'
      V  T  V  E  G  Q  L  E  G  G  S
>I3
5'-cggtaacggtagaaggccagctggaaggtggcggatcc-3'
   3'-attgccatcttccggtcgaccttccaccgcctaggccac-5'
      V  T  V  E  G  Q  L  E  G  G  G  S
>I4
5'-cggtaacggtagaaggccagctggaaggtggcggtggatcc-3'
   3'-attgccatcttccggtcgaccttccaccgccacctaggccac-5'
      V  T  V  E  G  Q  L  E  G  G  G  G  S
>I5
5'-cggtaacggtagaaggccagctggaaggtggcggtggcggatcc-3'
   3'-attgccatcttccggtcgaccttccaccgccaccgcctaggccac-5'
      V  T  V  E  G  Q  L  E  G  G  G  G  G  S
>E
5'-ggtggcggtggctcc-3'
    3'-cgccaccgaggccac-5'
    G  G  G  G  S
>T
5'-ggtggcttcagcacgcccgtctggataagccaggcgcaaggcatccgtg-3'
    3'-cgaagtcgtgcgggcagacctattcggtccgcgttccgtaggcacgac-5'
    G  G  F  S  T  P  V  W  I  S  Q  A  Q  G  I  R
```

B.

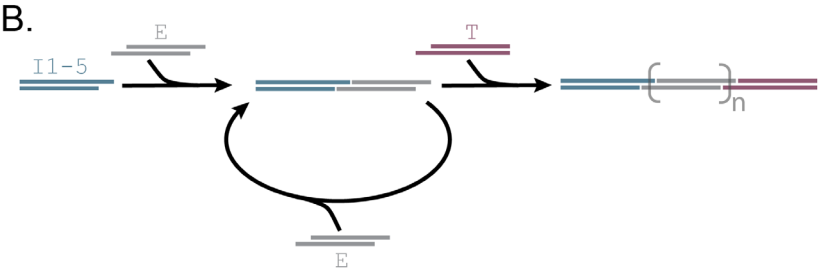

Figure S7. Assembly of oligonucleotides encoding linker sequences. **(A)** Oligonucleotide sequences encoding GS-linker polypeptides that connect Top7 and SecM17. Annealed double-stranded oligonucleotides are shown with the translated sequence below. The 3'- and C-terminal portion of Top7 encoded by the oligonucleotides are colored orange, the 5'- and N-terminal portion or SecM17 in red. **(B)** Scheme for generating fragments encoding linker sequences from 4 amino acids (n = 0, I1) to 28 amino acids (n = 4, I5) in length. Oligonucleotides I1 - I5 contain the 3'-terminal sequence of the Top7 ORF followed by a 4 nucleotide overhang. This overhang is complementary to one overhang of oligonucleotide E, allowing annealing of I1 - I5 to E. The other end of E can anneal to either E or T. Ligation of the annealed oligonucleotides yields fragments with 3-nuleotide overhangs that were ligated into the a plasmid backbone that allows expression of Top7-linker-SecM17-GFP fusion proteins.

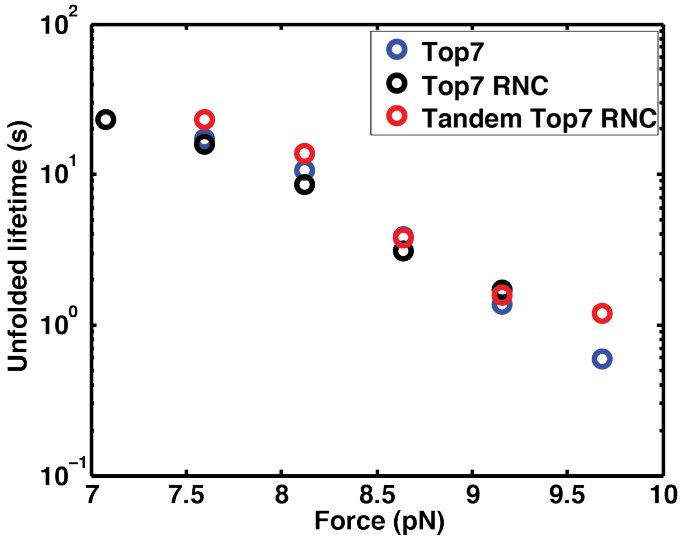

Figure S8. The ribosome does not influence folding of nascent Top7. Blue: Force-dependent folding lifetimes for Top7 (as shown in main figure 3D). Black: Ribosome-bound nascent Top7 with 100 aa between the C-terminus of Top7 and the P site peptidyl-tRNA. Red: Ribosome-bound nascent tandem Top7. For the tandem case, two Top7 domains have been translated, with 40 aa between the C-terminus of the C-terminal domain and the P site peptidyl-tRNA. The C-terminal domain is thus barely outside the ribosome exit tunnel. We do not observe a difference in folding rates for this construct compared to free Top7, despite its close proximity to the ribosome surface. Folding rates were calculated by modifying equation [10] (*19*) (originally prescribed for unfolding) (see Materials and Methods).

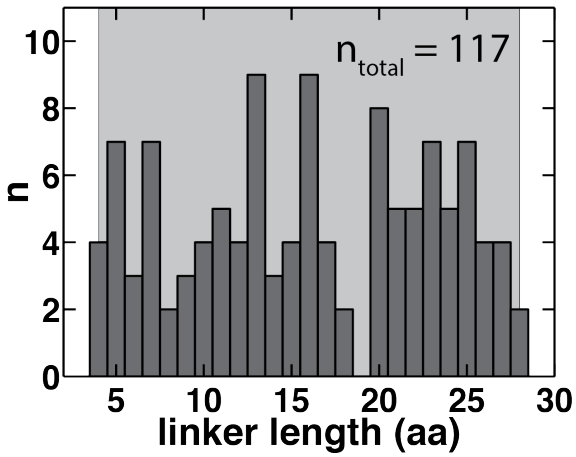

Figure S9. Sequencing plasmid DNA from colonies irrespective of whether or not they exhibited fluorescence recovered the entire distribution of linker lengths in the plasmid collection.

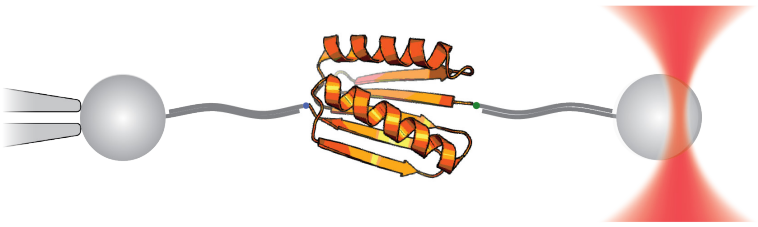

Figure S10. Experimental geometry for pulling experiments with single Top7 molecules. The structure of Top7 was obtained from PDB ID 1QYS.

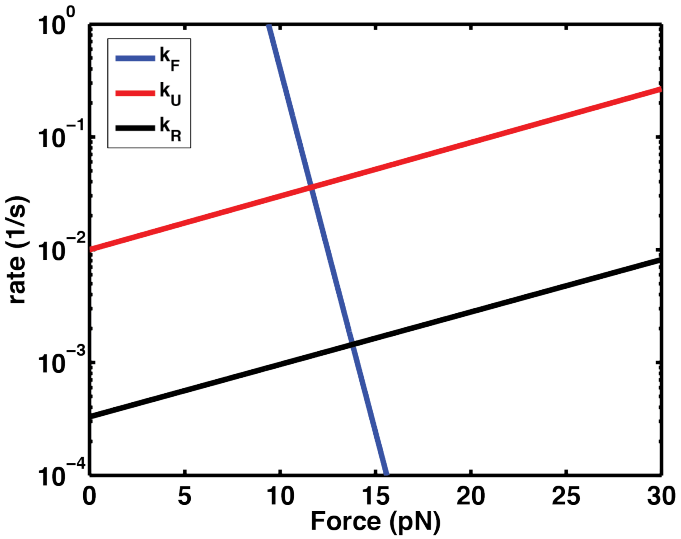

Figure S11. The force-dependent rates used in the kinetic scheme are plotted together. $k_N(F)$ and $k_U(F)$ were determined by Bell's model fits to the single-molecule data with the Top7 protein (Figure 3D). $k_R(F)$ was determined by a Bell's model fit to the single-molecule SecM restart data (Figure 1D). k_0 is the rate at zero-force (given by the intersection of the black line with the y-axis).

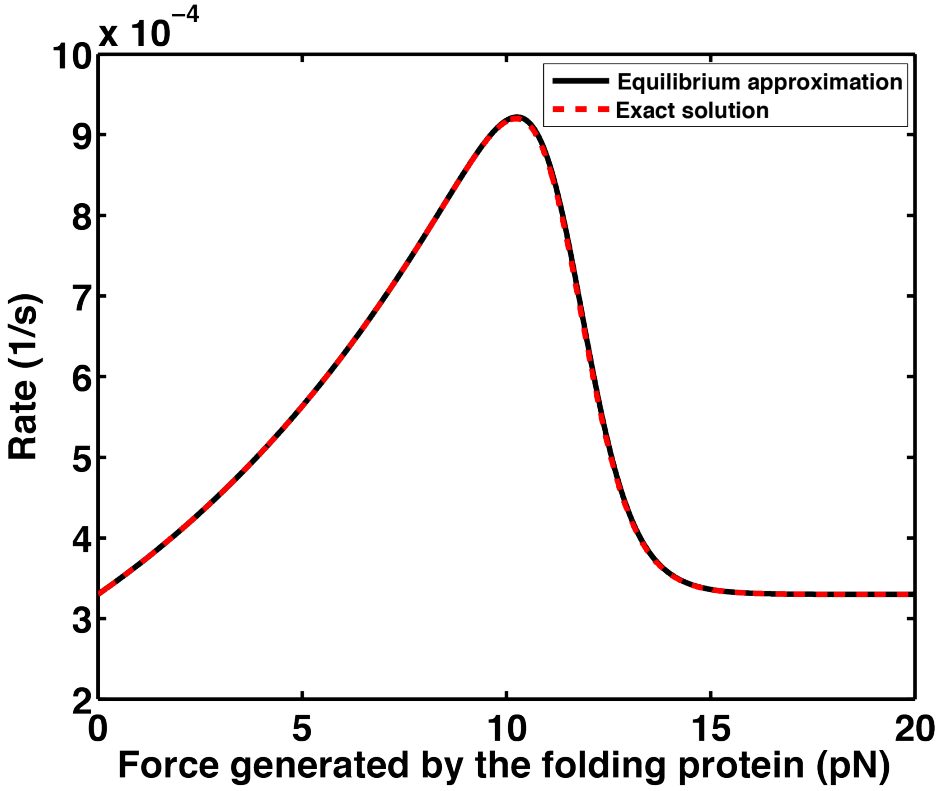

Figure S12. The effective restart rate as a function of force, $k_{Reff}(F)$, is a peaked distribution, with a maximum at ~10 pN.

References and Notes

1. D. A. Nissley, E. P. O'Brien, Timing is everything: Unifying codon translation rates and nascent proteome behavior. *JACS* **136**, 17892–17898 (2014). doi:10.1021/ja510082j

2. K. Ito, S. Chiba, Arrest peptides: Cis-acting modulators of translation. *Annu. Rev. Biochem.* **82**, 171–202 (2013). Medline doi:10.1146/annurev-biochem-080211-105026

3. Deutsch, in *Regulatory Nascent Polypeptides* (Springer, Tokyo, 2014), pp. 61–86.

4. D. N. Wilson, R. Beckmann, The ribosomal tunnel as a functional environment for nascent polypeptide folding and translational stalling. *Curr. Opin. Struct. Biol.* **21**, 274–282 (2011). Medline doi:10.1016/j.sbi.2011.01.007

5. A. Tsai, G. Kornberg, M. Johansson, J. Chen, J. D. Puglisi, The dynamics of SecM-induced translational stalling. *Cell Rep.* **7**, 1521–1533 (2014). Medline doi:10.1016/j.celrep.2014.04.033

6. H. Nakatogawa, K. Ito, The ribosomal exit tunnel functions as a discriminating gate. *Cell* **108**, 629–636 (2002). Medline doi:10.1016/S0092-8674(02)00649-9

7. J. Gumbart, E. Schreiner, D. N. Wilson, R. Beckmann, K. Schulten, Mechanisms of SecM-mediated stalling in the ribosome. *Biophys. J.* **103**, 331–341 (2012). Medline doi:10.1016/j.bpj.2012.06.005

8. M. N. Yap, H. D. Bernstein, The translational regulatory function of SecM requires the precise timing of membrane targeting. *Mol. Microbiol.* **81**, 540–553 (2011). Medline doi:10.1111/j.1365-2958.2011.07713.x

9. K. Nakamori, S. Chiba, K. Ito, Identification of a SecM segment required for export-coupled release from elongation arrest. *FEBS Lett.* **588**, 3098–3103 (2014). Medline doi:10.1016/j.febslet.2014.06.038

10. M. E. Butkus, L. B. Prundeanu, D. B. Oliver, Translocon "pulling" of nascent SecM controls the duration of its translational pause and secretion-responsive secA regulation. *J. Bacteriol.* **185**, 6719–6722 (2003). Medline doi:10.1128/JB.185.22.6719-6722.2003

11. C. M. Kaiser, D. H. Goldman, J. D. Chodera, I. Tinoco Jr., C. Bustamante, The ribosome modulates nascent protein folding. *Science* **334**, 1723–1727 (2011). Medline

12. J. P. Junker, F. Ziegler, M. Rief, Ligand-dependent equilibrium fluctuations of single calmodulin molecules. *Science* **323**, 633–637 (2009). Medline doi:10.1126/science.1166191

13. P. Nathans, Puromycin inhibition of protein synthesis: incorporation of puromycin into peptide chains. *Natl. Acad. Sci. U.S.A.* **51**, 585–592 (1964). doi:10.1073/pnas.51.4.585

14. H. Muto, H. Nakatogawa, K. Ito, Genetically encoded but nonpolypeptide prolyl-tRNA functions in the A site for SecM-mediated ribosomal stall. *Mol. Cell* **22**, 545–552 (2006). Medline doi:10.1016/j.molcel.2006.03.033

15. G. I. Bell, Models for the specific adhesion of cells to cells. *Science* **200**, 618–627 (1978). Medline doi:10.1126/science.347575

16. N. Ismail, R. Hedman, N. Schiller, G. von Heijne, A biphasic pulling force acts on transmembrane helices during translocon-mediated membrane integration. *Nat. Struct. Mol. Biol.* **19**, 1018–1022 (2012). Medline doi:10.1038/nsmb.2376

17. N. R. Voss, M. Gerstein, T. A. Steitz, P. B. Moore, The geometry of the ribosomal polypeptide exit tunnel. *J. Mol. Biol.* **360**, 893–906 (2006). Medline doi:10.1016/j.jmb.2006.05.023

18. B. Kuhlman, G. Dantas, G. C. Ireton, G. Varani, B. L. Stoddard, D. Baker, Design of a novel globular protein fold with atomic-level accuracy. *Science* **302**, 1364–1368 (2003). Medline doi:10.1126/science.1089427

19. O. K. Dudko, G. Hummer, A. Szabo, Theory, analysis, and interpretation of single-molecule force spectroscopy experiments. *Proc. Natl. Acad. Sci. U.S.A.* **105**, 15755–15760 (2008).doi:10.1073/pnas.0806085105 Medline

20. R. A. Maillard, G. Chistol, M. Sen, M. Righini, J. Tan, C. M. Kaiser, C. Hodges, A. Martin, C. Bustamante, ClpX(P) generates mechanical force to unfold and translocate its protein substrates. *Cell* **145**, 459–469 (2011). Medline doi:10.1016/j.cell.2011.04.010

21. M. E. Aubin-Tam, A. O. Olivares, R. T. Sauer, T. A. Baker, M. J. Lang, Single-molecule protein unfolding and translocation by an ATP-fueled proteolytic machine. *Cell* **145**, 257–267 (2011). Medline doi:10.1016/j.cell.2011.03.036

22. C. J. Woolstenhulme, S. Parajuli, D. W. Healey, D. P. Valverde, E. N. Petersen, A. L. Starosta, N. R. Guydosh, W. E. Johnson, D. N. Wilson, A. R. Buskirk, Nascent peptides that block protein synthesis in bacteria. *Proc. Natl. Acad. Sci. U.S.A.* **110**, E878–E887 (2013). Medline doi:10.1073/pnas.1219536110

23. S. Ude, J. Lassak, A. L. Starosta, T. Kraxenberger, D. N. Wilson, K. Jung, Translation elongation factor EF-P alleviates ribosome stalling at polyproline stretches. *Science* **339**, 82–85 (2013). Medline doi:10.1126/science.1228985

24. L. K. Doerfel, I. Wohlgemuth, C. Kothe, F. Peske, H. Urlaub, M. V. Rodnina, EF-P is essential for rapid synthesis of proteins containing consecutive proline residues. *Science* **339**, 85–88 (2013). Medline doi:10.1126/science.1229017

25. R. Shalgi, J. A. Hurt, I. Krykbaeva, M. Taipale, S. Lindquist, C. B. Burge, Widespread regulation of translation by elongation pausing in heat shock. *Mol. Cell* **49**, 439–452 (2013). Medline doi:10.1016/j.molcel.2012.11.028

26. B. Liu, Y. Han, S. B. Qian, Cotranslational Response to Proteotoxic Stress by Elongation Pausing of Ribosomes. *Mol. Cell* **49**, 453–463 (2013). Medline doi:10.1016/j.molcel.2012.12.001

27. P. De Los Rios, A. Ben-Zvi, O. Slutsky, A. Azem, P. Goloubinoff, Hsp70 chaperones accelerate protein translocation and the unfolding of stable protein aggregates by entropic pulling. *Proc. Natl. Acad. Sci. U.S.A.* **103**, 6166–6171 (2006). Medline doi:10.1073/pnas.0510496103

28. Lawless, *Statistical Models and Methods for Lifetime Data* (Wiley, Hoboken, NJ, ed. 2, 2003).

29. D. Sharma, D. R. Southworth, R. Green, EF-G-independent reactivity of a pre-translocation-state ribosome complex with the aminoacyl tRNA substrate puromycin supports an intermediate (hybrid) state of tRNA binding. *RNA* **10**, 102–113 (2004). Medline doi:10.1261/rna.5148704

30. J. B. Munro, M. R. Wasserman, R. B. Altman, L. Wang, S. C. Blanchard, Correlated conformational events in EF-G and the ribosome regulate translocation. *Nat. Struct. Mol. Biol.* **17**, 1470–1477 (2010). Medline doi:10.1038/nsmb.1925